APPLICATION OF A PROBABILISTIC METHOD FOR DETERMINATION OF THE THERMAL FIELD IN A FLAT-PLATE SOLAR COLLECTOR

ALICJA SIUTA-OLCHA

Lublin University of Technology, Faculty of Environmental Engineering
ul. Nadbystrzycka 40 B, 20-618 Lublin, Poland

ZASTOSOWANIE METODY PROBABILISTYCZNEJ DO WYZNACZANIA POLA TEMPERATUR W PŁASKIM KOLEKTORZE SŁONECZNYM

W pracy wykazano możliwość zastosowania metody Exodus do rozwiązywania problemów złożonej wymiany ciepła w płaskim kolektorze energii promieniowania słonecznego. Zostały opracowane modele probabilistyczne kolektora dla warunków ustalonych i nieustalonych. Opis matematyczny modeli został wyprowadzony z wykorzystaniem analogii między równaniami różnicowymi przewodzenia ciepła i równaniami opisującymi ruch cząstek błądzących. Wyniki obliczeń symulacyjnych temperatury pokrywy szklanej, płyty absorbera oraz czynnika wypływającego z kolektora według metody Exodus zostały porównane z wynikami uzyskanymi na podstawie metody zastępczej sieci cieplnej oraz metody różnic skończonych. Zastosowana procedura obliczeniowa umożliwia uwzględnienie w obliczeniach zmiennych warunków pogodowych i eksploatacyjnych instalacji słonecznej.

Summary

The Exodus method is applied to solve Fourier-Kirchoff's equation in heat transfer problems for flat plate solar collectors. Probabilistic models have been presented for the steady and non-steady conditions. The mathematical description of these models has been derived on the basis of the analogy between the conduction difference equation and the equation describing walking particle movement. The results of computations performed by the Exodus method have been compared to the results obtained by the Equivalent Thermal Network and the Finite Difference methods. The Exodus procedure allows the influence of changeable weather and operating conditions to be considered in calculations.

INTRODUCTION

The Exodus method is a statistical approach to the study of differential equations. It is one of methods for the approximate solution of heat transfer problems in real systems. This procedure enables relatively easy consideration of variability of material parameters depending on temperature and the analysis of all the boundary conditions applicable to the same boundary. The probabilistic techniques are specially recommended for determination of temperature changes at one or several nodes of a geometrical network.

The Exodus method has been modified and developed from the Monte Carlo method and makes use of an analogy between thermal conduction difference equations and probabilistic models of random walk processes. It is based on the concept of random walk of particles. A walking particle is not assigned to any weight or energy. It indicates a point which changes its position in a random way. Probabilistic methods enable us to determine the searched values with their specific maximum accuracy or probability allowing for non-linear thermal characteristics. As analytical methods of resolving thermal issues need many simplifications, they become less precise and experimental tests are more and more expensive.

This paper includes a proposal for the mathematical description of a thermal energy collector model operating in stationary and non-stationary conditions using the Exodus method. The proposal allows for random variability of meteorological and operational factors of the solar system which fundamentally determine the boundary conditions of complex heat transfer.

APPLICATION OF THE EXODUS METHOD TO RESOLVE PROBLEMS OF THERMAL CONDUCTION

The theoretical basis of Monte Carlo techniques, including the Exodus procedure and applications of these methods in various disciplines of science and engineering has been the subject of many publications [2–7]. The Exodus method is known to be able to resolve various issues related to thermal conduction. For example, it has been applied to determine the temperature distribution of periodically changing field and heat fluxes in a regenerator. In another case, the procedure was used to establish a relation between the gas temperatures and the temperatures of filling surface layers in a blast-furnace stove. The Exodus procedure has been mainly applied to resolve problems in radiant heat transfer.

The mathematical description of a thermal field with known initial and boundary conditions is also provided by the Fourier-Kirchoff differential equation of transient heat conduction. For solid non-stationary isotropic bodies and for isobaric processes, this equation is as follows [10]:

$$\rho \frac{\partial i}{\partial \tau} = \frac{\partial}{\partial x}\left(\lambda \frac{\partial T}{\partial x}\right) + \frac{\partial}{\partial y}\left(\lambda \frac{\partial T}{\partial y}\right) + \frac{\partial}{\partial z}\left(\lambda \frac{\partial T}{\partial z}\right) + \dot{q}_v. \tag{1}$$

Assuming that $\lambda = idem$ and $di = c_p \cdot dT$:

$$\frac{\partial T}{\partial \tau} = a\left(\frac{\partial^2 T}{\partial x^2} + \frac{\partial^2 T}{\partial y^2} + \frac{\partial^2 T}{\partial z^2}\right) + \frac{\dot{q}_v}{\rho \cdot c_p}. \tag{2}$$

The general solution of thermal conduction problems per Exodus procedure is received in the form of the following formula [5]:

$$T(x,y,z,\tau) = \frac{1}{M}\sum_{j=1}^{M} T_j. \tag{3}$$

Temperature $T(x, y, z, \tau)$ is the weighted average from temperatures at T_j boundary points. The T_j temperature may indicate:
-   point temperature at area boundary (boundary condition of the first type);
-   replacement temperature resulting from a known heat flux at area boundary

(boundary condition of the second type) or a known value of an internally active source of heat;

- temperature of fluid flowing round the considered area (boundary condition of the third type);
- gas or flame radiation temperature;
- temperature of any internal point, known from a previous series of walking particles motion.

The probability distribution of a particle subjected to principles of random behaviour should meet a given difference equation. The approximate distribution of random walk terminations at the boundary is the basis for general solution of a given case. The p_{ij} numbers defining the probability of walking particles transfer from i node to j node and the probability of particles remaining at p_{ii} node, should comply with the following axioms of probability:

$$- \bigwedge_{i,j} \qquad 0 \leq p_{ij} \leq 1, \tag{4}$$

$$- \bigwedge_{i} \qquad \sum_{j} p_{ij} < 1, \tag{5}$$

$$- \bigwedge_{i} \qquad 0 \leq p_{ii} \leq 1, \tag{6}$$

$$- \bigwedge_{i} \qquad p_{ii} + \sum_{j} p_{ij} = 1. \tag{7}$$

MODELING OF HEAT EXCHANGE PROCESSES IN SOLAR ENERGY COLLECTOR IN STEADY CONDITIONS

The considered heat model of a flat plate solar energy collector was in the form of a system of three homogeneous elements (Fig. 1), i.e. a glass cover, absorber plate and working fluid, with internal sources of heat emitted in the transparent face cover and in the surface layer of absorber plate.
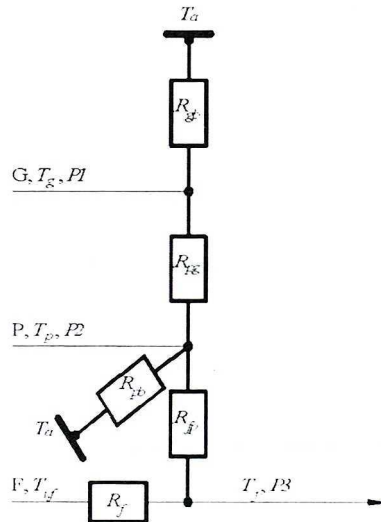

Fig. 1. Thermal network for a flat plate collector for steady conditions

To resolve the present problem, a well-defined section of the collector area was divided into isothermal difference elements. Difference equations were created recorded per Elementary Balance method for each distinct element. In accordance with this method, the sum of heat fluxes reaching the considered difference element from all neighboring nodes and the heat emitted by internal sources of heat amount to zero. The following system of equations was obtained [8]:

$$
\begin{cases}
Q_{bg} + Q_{pg} + P1 = 0 \\
Q_{gp} + Q_{fp} + Q_{bp} + P2 = 0 \\
Q_{pf} + (T_{f,i} - T_f) / R_f = 0
\end{cases}
\tag{8}
$$

The system of equations (8) was converted to the form allowing use of the Exodus procedure [8]:

$$
\begin{cases}
T_g - T_p \cdot p_{gp} = T_a \cdot p_{gb} + b_g \\
T_p - (T_g \cdot p_{pg} + T_f \cdot p_{pf}) = T_a \cdot p_{pb} + b_p \\
T_f - T_p \cdot p_{fp} = T_{f,i} \cdot p_f
\end{cases}
\tag{9}
$$

where:

$$
p_{gp} = \frac{R_{gb}}{R_{gb} + R_{gp}}
\tag{10}
$$

$$
p_{gb} = \frac{R_{gp}}{R_{gb} + R_{gp}}
\tag{11}
$$

$$
b_g = \frac{P1 \cdot R_{gb} \cdot R_{gp}}{R_{gb} + R_{gp}}
\tag{12}
$$

$$
p_{pg} = \frac{R_{pb} \cdot R_{pf}}{R_{pg} \cdot R_{pb} + R_{pg} \cdot R_{pf} + R_{pf} \cdot R_{pb}}
\tag{13}
$$

$$
p_{pf} = \frac{R_{pg} \cdot R_{pb}}{R_{pg} \cdot R_{pb} + R_{pg} \cdot R_{pf} + R_{pf} \cdot R_{pb}}
\tag{14}
$$

$$
p_{pb} = \frac{R_{pg} \cdot R_{pf}}{R_{pg} \cdot R_{pb} + R_{pg} \cdot R_{pf} + R_{pf} \cdot R_{pb}}
\tag{15}
$$

$$
b_p = \frac{P2 \cdot R_{pg} \cdot R_{pf} \cdot R_{pb}}{R_{pg} \cdot R_{pb} + R_{pg} \cdot R_{pf} + R_{pf} \cdot R_{pb}}
\tag{16}
$$

$$
p_{fp} = \frac{R_f}{R_{fp} + R_f}
\tag{17}
$$

$$
p_f = \frac{R_{fp}}{R_{fp} + R_f}
\tag{18}
$$

$$
P1 = I_c \cdot \alpha_g \cdot S_g
\tag{19}
$$

$$
P2 = I_c \cdot \tau_g \cdot \alpha_p \cdot S_p
\tag{20}
$$

$$P3 = \frac{T_{f,o} - T_{f,i}}{R_f}$$

(21)

and the equation of particle fraction behaviour satisfies:

$$\sum_j p_{ij} + p_{ib} = 1.$$

(22)

The p_{ij} numbers determine the probability of particle motion from i node to a neighboring node j and the p_{ib} numbers – the probability of walking particles motion from i node to the boundary of a known temperature. The p_f number indicates a probability of walking particles staying permanently in the **F** node without the possibility of continuing the motion. The value of p_{gp}, p_{gb}, p_{pg}, p_{pf}, p_{pb} probabilities depends mainly on meteorological parameters such as: ambient temperature, wind velocity and the relative humidity of the air. The value of b_g, b_p absolute terms depends, apart from the above mentioned factors, on the solar radiation. The change in working fluid flow intensity results in the change of p_f and p_{fp} probability values.

The visual model of walking particles distribution in the difference network applied to a segment of the collector area is shown in Figure 2. It illustrates the mechanism of particles motion starting from the **P** node representing the absorber plate.

In this case, the computational procedure is as follows:

1. The total number of walking particles start at the same time from a node of searched temperature, e.g. $M = 10^4$.

2. During the first cycle of walking, the particles are distributed in an organized way to neighboring nodes in the quantities resulting from conditions of heat transfer. The particles which, when walking, reach the boundaries of known temperatures are absorbed and become eliminated from further motion. The remaining particles return via determined directions to the node of the searched temperature.

3. During each successive cycle a smaller number of particles leave the starting node and the motion history is analogous to the first cycle.
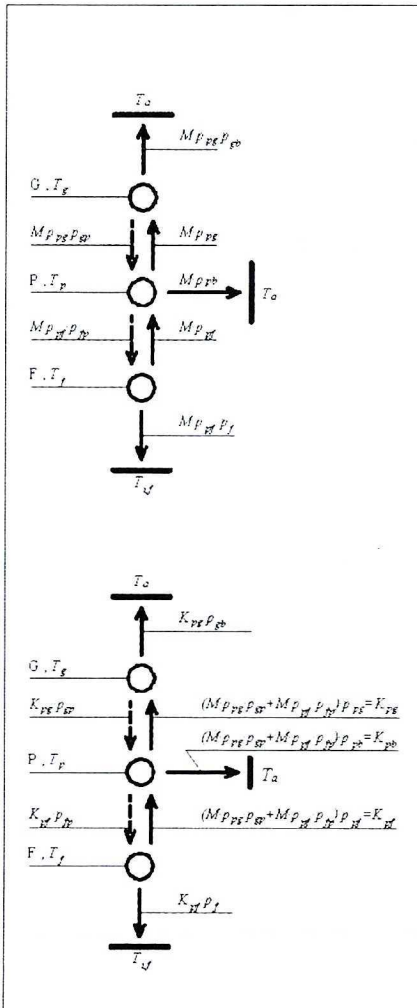

Fig. 2. Model of walking particles distribution for steady conditions

4. At the end of each cycle it is necessary to precisely determine:
    –   the total number of absorbed particles;
    –   the number of all particles passing through nodes in which internal heat sources are active;
    –   the number of particles which continue their motion from the concerned node.
5. The procedure expires when 99.99% of the total amount of particles is absorbed.

The solution for the issue of heat exchange in solar collector is presented in the form of the following formula:

$$T_i = (sk_b \cdot T_a + sk_f \cdot T_{f,i} + sk_g \cdot b_g + sk_p \cdot b_p) / M \tag{23}$$

MODELING OF HEAT TRANSFER PROCESSES IN SOLAR ENERGY COLLECTOR IN NON-STEADY CONDITIONS

To analyze the solar collector operation in non-steady conditions, the diagram of resistances and heat capacities for the previously distinguished nodes: **G**, **P** and **F** is presented in Figure 3.
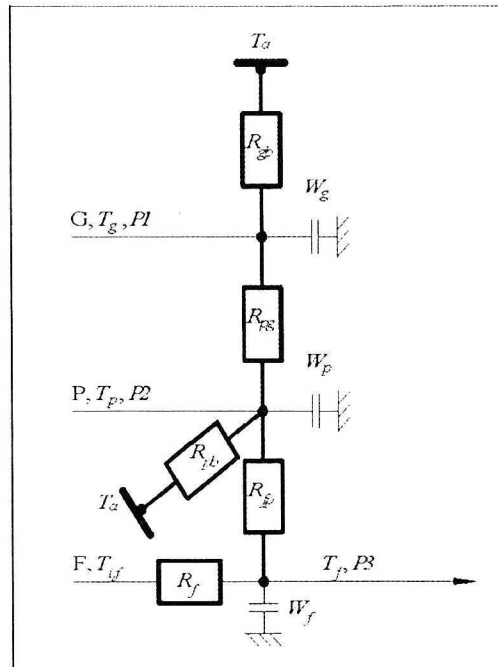

Fig. 3. Thermal network for a flat plate collector for non-steady conditions

The temporary energy balance for this i difference element in the stationary object can be expressed by the following formula [10]:

$$V_i \rho_i \frac{di_i}{d\tau} = \sum_j \dot{Q}_{ji} + \dot{Q}_{bi} + V_i q_{vi} \tag{24}$$

For the finite thermal capacity of the difference element when there are no transformations:

$$\frac{di_i}{d\tau} = c_{pi}\frac{dT_i}{d\tau} \tag{25}$$

The fluxes of heat flowing between the nodes were determined according to the temperature distribution at the beginning of the considered time interval. The partial first-order derivative of the time interval $d\tau$ was approximated using the forward difference diagram. This diagram allows the temperature at the end of the considered time interval to be determined.

Temperatures in particular nodes are calculated from the following system of equations:

$$\begin{cases} T_{g,\tau+1} = T_{g,\tau}\left[1-\frac{\Delta\tau}{W_g}\left(\frac{1}{R_{gb}}+\frac{1}{R_{gp}}\right)\right] + \frac{\Delta\tau}{W_g}\left(\frac{T_{p,\tau}}{R_{gp}}+\frac{T_a}{R_{gb}}+P1_\tau\right) \\[2mm] T_{p,\tau+1} = T_{p,\tau}\left[1-\frac{\Delta\tau}{W_p}\left(\frac{1}{R_{pb}}+\frac{1}{R_{pg}}+\frac{1}{R_{pf}}\right)\right] + \frac{\Delta\tau}{W_p}\left(\frac{T_{g,\tau}}{R_{pg}}+\frac{T_{f,\tau}}{R_{pf}}+\frac{T_a}{R_{pb}}+P2_\tau\right) \\[2mm] T_{f,\tau+1} = T_{f,\tau}\left[1-\frac{\Delta\tau}{W_f}\left(\frac{1}{R_{fp}}+\frac{1}{R_f}\right)\right] + \frac{\Delta\tau}{W_f}\left(\frac{T_{p,\tau}}{R_{fp}}+\frac{T_{f,i}}{R_f}\right) \end{cases} \tag{26}$$

The above system of equations was converted to the following form allowing the Exodus procedure to be introduced:

$$\begin{cases} T_{g,\tau+1} = T_{g,\tau}\cdot p_{gg} + T_{p,\tau}\cdot p_{gp} + T_a\cdot p_{gb} + b_{g,\tau} \\ T_{p,\tau+1} = T_{p,\tau}\cdot p_{pp} + T_{g,\tau}\cdot p_{pg} + T_{f,\tau}\cdot p_{pf} + T_a\cdot p_{pb} + b_{p,\tau} \\ T_{f,\tau+1} = T_{f,\tau}\cdot p_{ff} + T_{p,\tau}\cdot p_{fp} + T_{f,i}\cdot p_f \end{cases} \tag{27}$$

where:

$$p_{gg} = 1 - \frac{\Delta\tau}{W_g}\left(\frac{1}{R_{gp}}+\frac{1}{R_{gb}}\right) \tag{28}$$

$$p_{gp} = \frac{\Delta\tau}{W_g}\frac{1}{R_{gp}} \tag{29}$$

$$p_{gb} = \frac{\Delta\tau}{W_g}\frac{1}{R_{gb}} \tag{30}$$

$$b_{g,\tau} = \frac{\Delta\tau}{W_g}P1_\tau \tag{31}$$

$$p_{pp} = 1 - \frac{\Delta\tau}{W_p}\left(\frac{1}{R_{pb}}+\frac{1}{R_{pg}}+\frac{1}{R_{pf}}\right) \tag{32}$$

$$p_{pg} = \frac{\Delta\tau}{W_p}\frac{1}{R_{pg}} \tag{33}$$

$$p_{pf} = \frac{\Delta\tau}{W_p}\frac{1}{R_{pf}} \tag{34}$$

$$p_{pb} = \frac{\Delta\tau}{W_p}\frac{1}{R_{pb}} \tag{35}$$

$$b_{p,\tau} = \frac{\Delta\tau}{W_p}P2_\tau \tag{36}$$

$$p_{ff} = 1 - \frac{\Delta\tau}{W_f}\left(\frac{1}{R_{fp}} + \frac{1}{R_f}\right) \tag{37}$$

$$p_{fp} = \frac{\Delta\tau}{W_f}\frac{1}{R_{fp}} \tag{38}$$

and the following condition is met:

$$p_{ii} + \sum_j p_{ij} + p_{ib} = 1. \tag{39}$$

After each time interval the change in values of p_{ii}, p_{ij} and p_{ib} probabilities was considered. This is caused by a change in thermal resistance values resulting from variable weather and operation conditions during solar energy collector operation. Climate parameters such as ambient temperature, wind velocity, relative air humidity affect the values of p_{gg}, p_{gb}, p_{pp} and p_{pb} probabilities. The solar radiation intensity determines the values of b_g and b_p absolute terms. The values of p_{ff} and p_f probabilities depend on the value of volume flow rate of working fluid.

To maintain the physical correctness of the obtained system difference equations (27), the time interval was chosen in such a way that the values of p_{ii} properties are never negative. At the same time the physical correctness of equations ensures stability and solution convergence.

Interpretation of the probabilistic model for non-steady conditions for two first time intervals is shown in Figure 4. It presents the history of walking particles passes starting from the **F** node which represents the working fluid in the collector.

To solve the problem, the following strategy was invoked:

1. At the beginning it was assumed that the temperature profile for the collector area at the initial time τ is known and the boundary temperatures, the capacity of the internal thermal sources, the convective heat transfer coefficient on the boundary of particular elements are known.

2. During the first time interval, i.e. at the moment $\tau + n\cdot\Delta\tau$, where $\Delta\tau$ is a time interval of one-second duration and n is
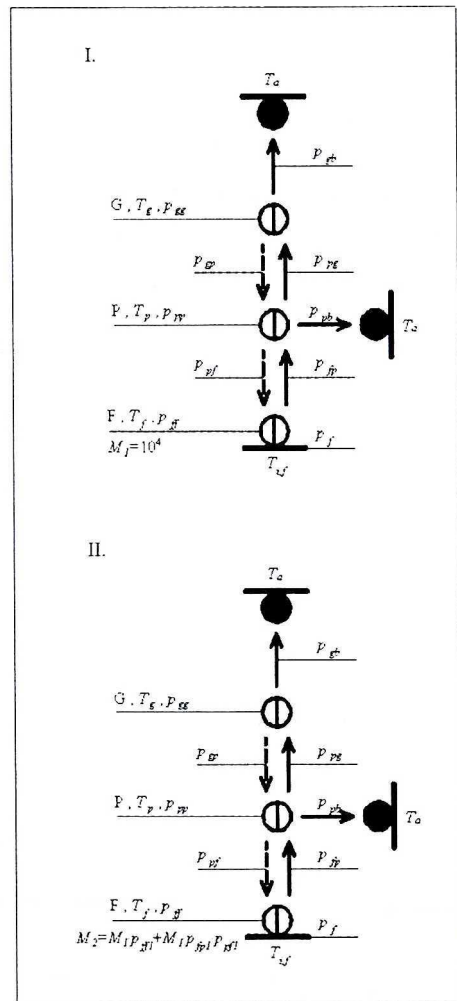

Fig. 4. Model of walking particles distribution for non-steady conditions

the number of intervals, the 10^4 ($= M$) walking particles start from the node of searched temperature. Some particles remain during this interval in the considered node and the others walk in specific directions to neighboring nodes. Also an appropriate number of particles remain in each of these nodes. The particles which reach the absorbing boundaries do not participate in further passes. Some particles return from various directions to the **F** node.

3. During each successive interval, an appropriate number of particles pass to the plane of the lower time moment number.
4. After each time interval the following was recorded:
   - number of particles passing through neighboring nodes per prepared scheme;
   - number of particles which reached the time boundary;
   - number of particles continuing their motion from the **F** node;
   - total number of particles eliminated from motion at the boundary of known ambient temperature T_a and at the absorbing boundary of known temperature $T_{f,i}$.
5. The procedure expires at the time of reaching the time plane τ or at the geometrical boundary of the area of known temperature.

The value of searched temperature in any node of the network and at any time for the considered area of collector may be determined from the following formula:

$$T_{i,\tau + n\Delta\tau} = \left(sk_b \cdot T_a + sk_f \cdot T_{f,i} + sk_\tau \cdot T_{i\tau} + sk_g \cdot b_g + sk_p \cdot b_p\right) / M. \tag{40}$$

RESULTS AND DISCUSSION

The analysis was performed for a flat-plate solar collector with the parameters presented in Table 1. The Thermal_Resistance.PAS program was used to carry out an analysis of the solar energy collector in the steady conditions (author of this program – Siuta-Olcha).

Table 1. Construction and material parameters of the collector

Parameter	Description
Dimensions: length × width, [mm]	1350 × 1140
Gross area of collector, [m²]	1.546
Aperture area of collector, [m²]	1.417
Absorber area of collector, [m²]	1.2
Glass cover thickness, [mm]	4
Absorber plate thickness, [mm]	1.4
Back insulation thickness, [mm]	38
Collector box thickness, [mm]	1
Tube diameter, [mm]	8.9
Number of transparent covers	1
Glass transmittance	0.80
Absorber plate absorptance	0.95

Temperature calculations for glass cover, absorber plate and working fluid flowing out of the collector were performed on the basis of matrix computation and the Exodus procedure. Table 2 specifies temperature values of working fluid flowing out of the collector obtained from measurements and calculations, computed by the Equivalent

Thermal Network method (*ETNM*) [1], the matrix method (*MM*) and the Exodus method (*EX*). Figure 5 shows the efficiency curve for the investigated flat-plate solar collector versus reduced temperature difference $(T_{f,o}-T_a)/I_c$. Figure 6 illustrates i) changes of useful energy flux gained by 1 m² collector surface, ii) the influence of solar irradiance on thermal efficiency on the assumption the constant value of mean surplus of medium temperature over ambient temperature. A detailed analysis of the influence of weather parameters (I_c, T_a, v_w) and exploitation parameters $(Q, T_{f,i})$ on thermal efficiency of solar collectors of various constructions was presented in [8, 9].

Table 2. Selected results of measurements and calculations for the collector in the steady conditions

| No.	I_c [W/m²]	Q [m³/s]	v_w [m/s]	T_a [°C]	$T_{f,i}$ [°C]	$T_{f,omeasur}$ [°C]	$T_{f,oETNM}$ [°C]	$\delta 1$ [%]	$T_{f,oMM}$ [°C]	$T_{f,oEX}$ [°C]	$\delta 2$ [%]
1.	330	6.667e-6	3.5	13.6	23.9	31.4	30.5	2.87	31.6	31.6	-0.60
2.	460	2.833e-5	3.0	13.4	16.8	20.8	19.6	5.77	20.1	20.1	3.36
3.	505	4.833e-5	1.5	9.7	13.2	15.9	15.0	5.66	15.3	15.3	3.77
4.	560	7e-5	0	32.9	24.5	27.2	26.4	2.94	26.3	26.3	3.31
5.	780	2.833e-5	1.0	29.0	26.1	32.8	31.5	3.96	32.0	32.0	2.44
6.	800	4.5e-5	1.0	32.4	25.1	29.4	29.1	1.02	29.0	29.0	1.36
7.	800	1.667e-5	1.0	32.4	30.0	38.0	39.6	-4.21	40.0	40.0	-5.26
8.	820	1e-5	0	28.7	33.0	45.0	49.2	-9.33	49.0	49.0	-8.89
9.	825	1.333e-5	1.0	34.1	32.2	40.8	45.0	-10.29	44.9	44.9	-10.05
10.	860	4e-5	2.0	29.1	23.7	29.2	28.5	2.40	28.4	28.4	2.74
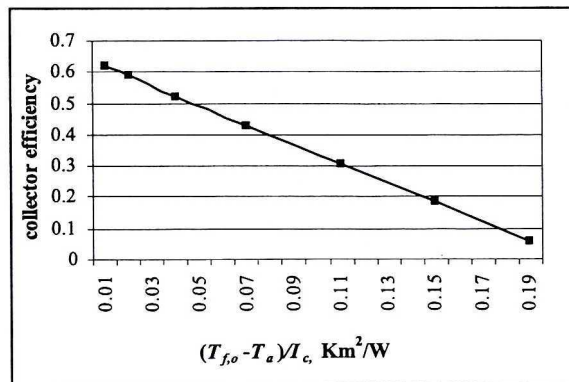
Fig. 5. The collector efficiency versus reduced temperature difference

    An analysis of the solar energy collector in the non-steady conditions was carried out using the STAN_NU.PAS program (author of this program – Siuta-Olcha). The calculations of temperature in three selected nodes of the collector were performed by the difference method based on the scheme shown and on the basis of the Exodus procedure. Selected results of calculations for the flat-plate solar energy collector at subsequent moments of time are included in Table 3.
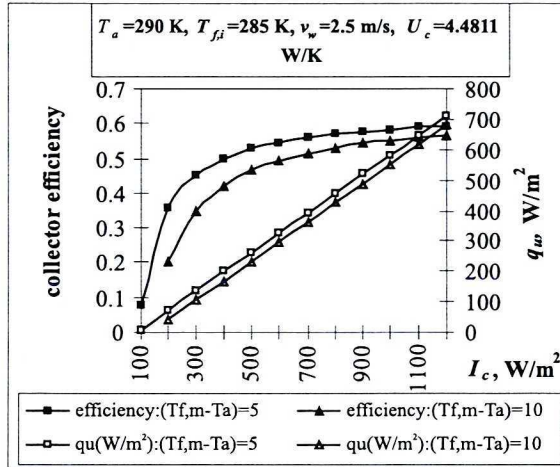
Fig. 6. The influence of solar irradiance on thermal efficiency of the collector and on useful energy flux

Table 3. Selected calculation results for the collector in the non-steady conditions

No.	τ [s]	T_{gEX} [°C]	T_{gFDM} [°C]	$\delta 1$	T_{pEX} [°C]	T_{pFDM} [°C]	$\delta 2$	$T_{f,oEX}$ [°C]	$T_{f,oFDM}$ [°C]	$\delta 3$
$I_c = 600$ W/m², $T_a = 10$°C, $v_w = 2$ m/s, $Q = 10^{-5}$ m³/s, $T_{f,i} = 12$°C
1.	0	10.50	10.50	-	12.00	12.00	-	11.0	11.0	-
2.	60	10.76	10.75	0.09	16.00	16.50	3.03	14.4	14.1	-2.13
3.	180	11.30	11.30	-	20.60	21.20	2.83	18.8	18.7	-0.53
4.	300	11.90	11.90	-	22.90	23.50	2.55	21.1	20.9	-0.96
5.	420	12.40	12.40	-	24.10	24.70	2.43	22.3	22.1	-0.90
6.	600	12.90	12.90	-	24.90	25.50	2.35	23.1	22.8	-1.31
7.	720	13.20	13.20	-	25.10	25.70	2.33	23.3	23.1	-0.86
8.	900	13.40	13.50	0.74	25.30	25.90	2.32	23.4	23.2	-0.86
9.	1200	13.60	13.70	0.73	25.40	25.97	2.19	23.5	23.3	-0.86
10.	1500	13.70	13.80	0.72	25.41	25.99	2.23	23.6	23.3	-1.29
11.	1800	13.80	13.90	0.72	25.42	26.00	2.23	23.6	23.3	-1.29
$I_c = 700$ W/m², $T_a = 25$°C, $v_w = 2$ m/s, $Q = 10^{-5}$ m³/s, $T_{f,i} = 20$°C
No.	τ [s]	T_{gEX} [°C]	T_{gFDM} [°C]	$\delta 1$	T_{pEX} [°C]	T_{pFDM} [°C]	$\delta 2$	$T_{f,oEX}$ [°C]	$T_{f,oFDM}$ [°C]	$\delta 3$
1.	0	27.00	27.00	-	27.10	27.10	-	27.00	27.00	-
2.	60	27.05	27.05	-	30.60	30.30	-0.99	28.50	28.60	0.3
3.	180	27.20	27.20	-	33.60	33.20	-1.20	31.30	31.40	0.3
4.	300	27.40	27.40	-	35.10	34.65	-1.30	32.70	32.80	0.3
5.	420	27.60	27.60	-	35.80	35.40	-1.10	33.35	33.50	0.4
6.	600	27.85	27.87	0.07	36.30	35.90	-1.10	33.80	34.00	0.6
7.	720	27.95	27.97	0.07	36.40	36.00	-1.10	33.90	34.10	0.6
8.	900	28.10	28.10	-	36.50	36.10	-1.10	34.00	34.20	0.6
9.	1200	28.15	28.16	0.04	36.54	36.15	-1.10	34.00	34.30	0.9
10.	1500	28.19	28.19	-	36.55	36.16	-1.10	34.00	34.30	0.9

The heating curves (Fig. 7) representing distinguished elements of solar collector make the determination of the three time constants possible. The collector time constant is a basic dynamic parameter of the solar system. Fig. 8 presents the dependence of a medium time constant on collector thermal resistances in relative values. The thermal resistance of the fluid has the most important influence on its heating up dynamics. Fig. 9 shows the influence of heat capacities on the fluid time constant in relative values.
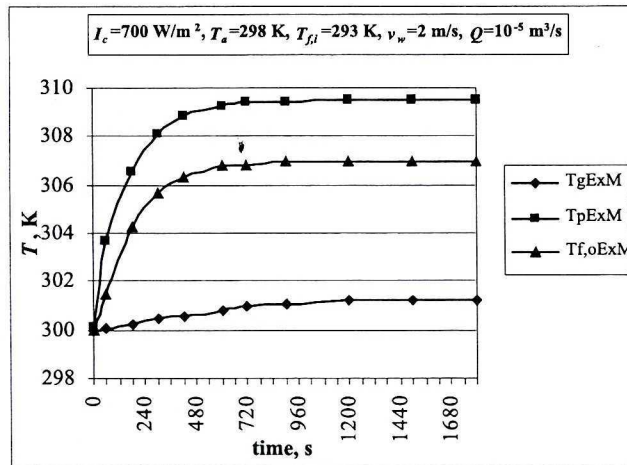

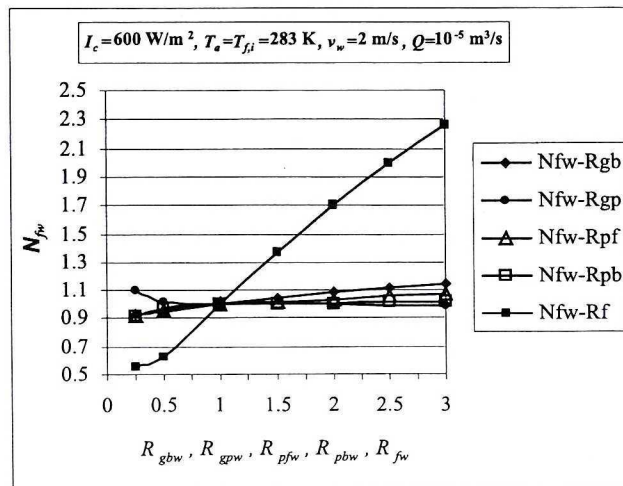Fig. 7. Heating curves of solar collector

Fig. 8. The influence of thermal resistances on the fluid time constant in relative values
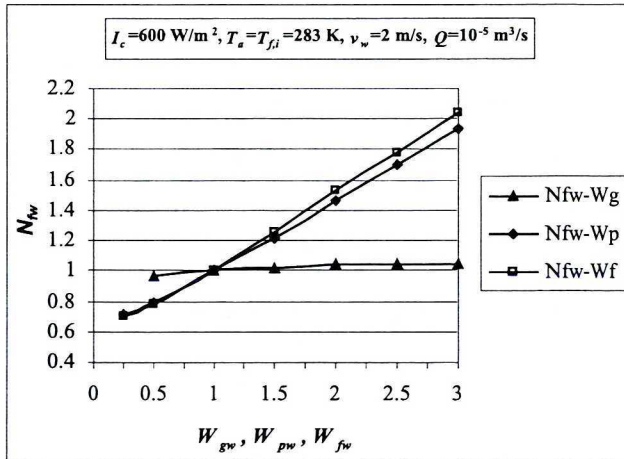
Fig. 9. The influence of heat capacities on the fluid time constant in relative values

CONCLUSIONS

Generally it is not possible to obtain the solution of the thermal conduction equation for practical cases by using the analytical method and thus the numerical method was applied to calculations. The problem of heat conduction with internal heat sources and non-linear boundary conditions has been solved. To determine the thermal field in a flat plate solar collector, the Exodus procedure was applied. First of all, it allows for calculation of the temperature of fluid flowing out of the collector with high accuracy. The calculated results make it possible to i) analyze the collector operation under any conditions, ii) evaluate the energetic efficiency of its operation and iii) check the heat dynamics of homogeneous elements of the collector. On the basis of these data it is then possible to determine the effective heat flow received from 1 m² of collector area and to determine its heat efficiency.

The numerical modeling of heat processes occurring during operation of the collector has, as its goal, their optimization for the purpose of designing, controlling and economical testing of solar systems.

NOMENCLATURE

c_p — fluid specific heat at constant pressure, $[J/(kg \cdot K)]$;

F — isothermal node, characteristic for working fluid;

G — isothermal node, characteristic for face cover glass;

i — specific enthalpy, J/kg;

I_c — global solar irradiance on collector plane, $[W/m^2]$;

M — total number of walking particles starting from the i node, i.e. the node of determined temperature, $[-]$;

P — isothermal node, characteristic for absorber plate;

p_{ij}	–	transition probability of walking particles from i node to j node, [-];
$P1$	–	thermal energy emitted in glass cover in the middle of its thickness, [W];
$P2$	–	thermal energy emitted on absorber plate surface, [W];
$P3$	–	heat transferred by absorber to working fluid, [W];
Q	–	volume flow rate of heat transfer fluid, [m³/s];
$\dot{Q}_{ji}$	–	thermal flux reaching i node from neighboring j node, [W];
q_u	–	useful energy gain from collector, [W/m²];
$\dot{q}_v$	–	volumetric capacity of heat source, [W/m³];
R_f	–	thermal resistance of working fluid, [K/W];
R_{ij}	–	thermal resistance between difference element with i node and differential element with j node, [K/W];
S_p	–	absorber plate area, [m²];
S_c	–	collector area, [m²];
S_g	–	glass cover area, [m²];
sk_p	–	total number of walking particles passing through the **P** node in which the internal source of heat with $P2$ power is active, [-];
sk_f	–	total number of walking particles absorbed at the boundary, equated with the boundary of known temperature of fluid flowing to collector $T_{f,i}$, [-];
sk_b	–	total number of walking particles eliminated at the boundary contacting outside air of known temperature T_a, [-];
sk_g	–	total number of walking particles passing through the **G** node in which the internal source of heat with $P1$ power is active, [-];
sk_τ	–	number of walking particles which started their motion in the i node and finished it in the time plane τ of known initial temperature $T_{i,\tau}$ of a given node, [-];
$T_{f,i}$	–	inlet fluid temperature, [K];
$T_{f,o}$	–	outlet fluid temperature, $T_{f,o} = T_f$, [K];
T_i	–	temperature of solar collector element with characteristic i node, [K];
T_a	–	ambient temperature, [K];
V	–	volume, [m³];
v_w	–	wind velocity, [m/s];
W	–	heat capacity, [J/K];
x, y, z	–	coordinates.

Greek symbols

α	–	absorptance of solar radiation, [-];
$\Delta\tau$	–	time interval, [s];
λ	–	thermal conductivity, [W/m·K)];
ρ	–	density, [kg/m³];
τ	–	transmittance of solar radiation, [-].

Subscripts

b	–	boundary;
f	–	fluid;
g	–	glass;
p	–	plate.

REFERENCES

[1]   Chochowski A.: *Wymiana ciepła w płaskich cieczowych kolektorach słonecznych, cz. II, Badania i obliczenia*, Roczniki Nauk Rolniczych, **79-C-1**, 217–222 (1990).
[2]   Emery A.F., W.W. Carson: *A modification to the Monte Carlo Method – The Exodus method*, Journal of Heat Transfer, Transactions of the ASME, **90**(8), 328–332 (1968).
[3]   Howell J.R., M. Perlmutter: *Monte Carlo Solution of Thermal Transfer Though Radiant Media Between Gray Walls*, Journal of Heat Transfer, Transactions of the ASME, **86**(2), 116–122 (1964).
[4]   King G.W.: *Monte Carlo Method for Solving Diffusion Problems*, Industrial and Engineering Chemistry, **43**(11), 2475–2478 (1951).
[5]   Minkowycz W.J., E.M. Sparrow, G.E. Schneider, R.H. Pletcher: *Handbook of numerical heat transfer*, John Wiley & Sons, New York 1988, 673–722.
[6]   Sadiku M.N.O., D.T. Hunt: *Solution of Dirichlet problems by the Exodus method*, IEEE Transactions on Microwave Theory and Techniques, **40**(1), 89–95 (1992).
[7]   Sadiku M.N.O., S.O. Ajose, F. Zhibao: *Applying the Exodus Method to solve Poisson's Equation*, IEEE Transactions on Microwave Theory and Techniques, **42**(4), 661–666 (1994).
[8]   Siuta-Olcha A.: *Ocena jakościowa płaskich cieczowych kolektorów słonecznych na podstawie procedury probabilistycznej*, Inżynieria i Ochrona Środowiska, Częstochowa, **7**(2), 209–225 (2004).
[9]   Siuta-Olcha A.: *Efficiency characteristics of flat-plate solar collector*, [in:] Proceedings of the Second National Congress of Environmental Engineering, Lublin, Poland, September 4–8, 2005, Environmental Engineering, Taylor & Francis Group, London 2007, 479–483.
[10] Szargut J.: *Modelowanie numeryczne pól temperatury*, WNT, Warszawa 1992.